

y3. N21/5. 8/517

TECHNICAL MEMORANDUMS

NATIONAL ADVISORY COMMITTEE FOR AERONAUTICS

No. 517

University of Maryland  
Glenn L. Martin College  
of Engineering and Aero-  
nautical Sciences  
Library

INVESTIGATION OF THE EFFECT OF THE FUSELAGE ON  
THE WING OF A LOW-WING MONOPLANE

By H. Muttray

From Luftfahrtforschung, June 11, 1928

Washington  
June, 1929

NATIONAL ADVISORY COMMITTEE FOR AERONAUTICS.

TECHNICAL MEMORANDUM NO. 517.

INVESTIGATION OF THE EFFECT OF THE FUSELAGE ON  
THE WING OF A LOW-WING MONOPLANE.

By H. Muttray.

Summary

The mutual action of wing and fuselage, which greatly affects the construction of airplanes, is dealt with in the present report.

A certain number of systematic wind-tunnel tests were made in order to elucidate the question. For example, there will be shown what effect the distance between the wing and the nose of the fuselage, measured along the fuselage axis, has on the position of the fuselage with respect to the wing.

Other tests deal with the transition from fuselage to wing root, which, if inadequate on low-wing monoplanes, may become dangerous by causing the air flow to separate at the wing root.

Lastly, reference is made to the mutual interference of wing and fuselage for various wing shapes. In this connection, tapered wings, rectangular wings and wings with a cutaway in the trailing edge are discussed.

---

\* "Untersuchungen über die Beeinflussung des Tragflügels eines Tiefdeckers durch den Rumpf." From Luftfahrtforschung, June 11, 1928, pp. 33-39.

### Introduction

When a fuselage is combined with a given wing, we expect the polars of the "wing-and-fuselage" group to come nearest to the best value, which is usually that of the polar of the wing alone. The difference between the polars affords a means of estimating the effect of the fuselage on the wing.

The mutual interference depends chiefly on the following items:

1. Fuselage position (high-wing or low-wing monoplane), distance between wing and nose of the fuselage;
2. Dimensions of fuselage, especially length and width;
3. Shape of fuselage, e.g., the cross section and the shape of the nose.

The effect of the fuselage on the wing is manifestly the least when the fuselage acts the same as the wing portion which it replaces. This occurs when the following conditions are satisfied:

- a) The air flow at the wing root (the portion of the wing close to the fuselage) is not unfavorably affected by the fuselage and does not separate from the surface;
- b) The lift of the fuselage is not smaller than that of the wing portion it replaces;
- c) The lift of the fuselage acts at the center of pressure of the wing.

An additional induced drag is produced when, owing to an unsuitable choice of the above three geometrical values, the fuselage lacks the requisite properties. Thus, in the case of the approximately elliptic lift distribution over the wing alone, a hollow may develop in place of the fuselage and produce an additional induced drag, as well as a decrease in the maximum lift (Fig. 1).

An investigation regarding the effect of the height of the fuselage with reference to the wing (high-wing or low-wing monoplane) was published in Report I of the *Ergebnisse der Aerodynamischen Versuchsanstalt zu Göttingen*, p. 118 ff.). The low-wing arrangement proved less satisfactory than the high-wing. The differences are immaterial with normal fuselage shapes, provided case E of the above reference is disregarded. This case deals with a low-wing monoplane of which the wing is located at a distance below the fuselage approximately equal to the thickness of the wing section.

The increased effect on the polar, when the fuselage is located on the upper surface of the wing, must be attributed to the great sensitivity of this surface. The air flow, subjected to a great increase in pressure above the rear portion of the wing, is easily disturbed by small obstacles, such as bumps, roughness, etc., and soon separates at large angles of attack. Besides, in the case of the wing alone, the flow begins to separate from the center of the wing at large angles

of attack. This tendency can, of course, be easily increased by the fuselage. All the following investigations are therefore based on the low-wing arrangement, which is considered aerodynamically less favorable.

### T e s t   R e s u l t s

#### Series I.

##### Wing with a Disk in Place of the Fuselage

In order to show that a wing polar is unfavorably affected even by an "ideal fuselage," a thin, vertical disk with well-sharpened edges was placed over the center of the wing (Fig. 2). The disk represents only the friction effect of the left and right vertical sides of the fuselage.

The wing was rectangular with a chord of 25 cm, and an aspect ratio of 5. The wing section used was a Göttingen 426. The shape of the disk, which was 2 mm thick, is shown in Fig. 2. The air speed was  $v = 30 \text{ m/s}$ .

In each case the evaluation of the test results was carried out in the usual way.

$$c_a = \frac{A}{q F}, \quad c_w = \frac{W}{q F}, \quad c_m = \frac{M}{q F t} .$$

A is the measured lift in kg;

W, the measured drag in kg;

M, the moment measured about the "datum axis" in mkg.

(The "datum axis" is the transverse axis through the

foremost point of the chord of the largest wing section. Also see the definition in Report I of the Ergebnisse der Aerodynamischen Versuchsanstalt zu Göttingen, page 32);

$F$ , the datum area in  $m^2$ , i.e., in each case the area of the wing alone;

$t$ , the maximum wing chord in meters;

$q = \frac{\rho}{2} v^2$ , the dynamic pressure in  $kg/m^2$ ;

$\rho$ , the density of the air in  $\frac{kg \ s^2}{m^4}$ ;

$v$ , the air speed in  $m/s$ ;

$c_a, c_w$ , the air-force coefficients;

$c_m$ , the moment coefficient.

The polars (Fig. 3) show an obvious increase in drag with increasing lift and a decrease in the maximum lift after the disk is put in place. The flow is retarded by friction against the disk surfaces. This probably occurs especially along the line of intersection of the upper surface of the wing and the disk, where two boundary layers meet.

## Series II.

### Wing at Various Distances from the Nose of the Fuselage

The magnitude of the additional drag is greatly affected by the distance between the wing and the nose of the fuselage. The model for a corresponding series of tests is shown in Figure 4.

The rectangular fuselage (height 12 cm, maximum width 10 cm) covers one-tenth of the span of the wing of aspect ratio 5 and

section No. 426. The nose of the fuselage forms half an ellipse as seen from above and is rectangular as seen from the side. The major half-axis of the ellipse has approximately the length of the wing chord and the minor half-axis is equal to one-half the fuselage width. The long tapering rear portion of the fuselage, which is symmetrical with respect both to the horizontal and to the vertical longitudinal plane, ends in a vertical edge. The distance of the leading edge of the wing from the nose of the fuselage, in terms of the wing chord, is

1.50	in position I,
0.95	" " II,
0.50	" " III,
0.22	" " IV.

The polars are plotted in Figure 5. Curve 1 characterizes the wing alone and curve 2, the wing and fuselage for the maximum distance of the wing. The maximum of curve 2 lies above that of the wing alone. Hence the fuselage exerts a greater lift than the portion of the wing which it replaces.

Curve 2 coincides approximately with curve 3, which corresponds to a distance roughly equal to the wing chord. Both polars compared with that of the wing alone show an increase in drag with increasing lift. The moment curves, compared with that of the wing alone, are shifted forward.

There is a definite relation between the shifting of the moment curves and the increase in drag with increasing lift.

The changed position of the center of pressure shows that the fuselage lift does not apply at the wing portion replaced by the fuselage and that a depression must have occurred in the lift distribution over the wing. The additional induced drag is a result of this depression.

In the case of curve 4, corresponding to a distance of the wing equal to 0.5 of the chord, the moment curve agrees fairly well with that of the wing alone. Hence, there is no reason for an additional induced drag. Except for its upper portion, there is actually only a parallel displacement of polar 4 with respect to that of the wing alone, although in its lower portion the additional induced drag exceeds that of the polar for the maximum wing distance.

At  $c_a = 1.15$  the sharp nose of the fuselage causes the flow to separate at the wing root. From this point the polar is strongly deflected toward the right.

Curve 5 for the smallest distance of the wing coincides with curve 4 for small lift values and hence also has a very substantial additional drag. Between  $c_a = 0.3$  and  $c_a = 0.95$  the additional induced drag increases from 0.14 to 0.2. From this point the nose of the fuselage again causes the flow to separate at the wing root and the curve bends suddenly and sharply to the right.

## Series III.

## Rectangular and Tapered Wings with the Same Fuselage

For the purpose of investigating the influence exerted on the flow at the wing root, we will now reverse our method. Thus we shall first fit a rectangular and then a tapered wing to the same fuselage, both wings having the same section, area, and aspect ratio.

The rectangular wing is the one used in the second series of tests. The tapered wing has a maximum chord of 30 cm, and a minimum chord of 10 cm. The shape and arrangement of the fuselage are shown in Figures 6 and 7. The fuselage has a long, well-rounded nose. The rear end of the fuselage is strongly tapered.

The polars are shown in Figure 8. In connection with the moment line it should be noted that the moment datum points of the rectangular and of the tapered wings are not coincident on the model.

The polars show that the additional drag due to the fuselage is approximately the same for both wings up to  $c_a = 0.7$ , whereas, in the upper portion of the polars the model with rectangular wings is considerably less favorable. The difference of the maximum lifts between the polars for the wing alone and for the wing and fuselage together is considerably smaller with a tapered wing than with a rectangular wing. Hence, aerodynamically, the tapered wing is not so unfavorably affected by the fuselage as

the rectangular wing. This may be accounted for by the fact that, in the case of the tapered wing, the fuselage is smaller in comparison with the root section of the wing than in the case of the rectangular wing.

#### Series IV.

##### Variation of the Angle between the Wing and the Side of the Fuselage

It was stated in the introduction that an unfavorable shape of the fuselage may easily cause the flow to separate at the wing root. An unsuitable shape of the fuselage nose may produce this phenomenon when, as already shown in the second series of tests, the nose of the fuselage is very close to the leading edge of the wing. This fact is confirmed by tests which were published in Report III of the Ergebnisse der Aerodynamischen Versuchsanstalt zu Göttingen, page 115. It was then shown that blunt-nosed engine nacelles caused the flow to separate prematurely and hence to produce a high induced drag similarly to cutaway portions of the leading edge.

In the present series of tests it will be shown that similar phenomena may be produced by altering the angle between the wing and the right and left sides of the fuselage. In practice there may be an acute angle between the wing and the side of the fuselage, when the latter has an elliptic cross section and is situated above the wing.

The rectangular wing, which has been used for the foregoing series of tests, was in turn provided with a square fuselage and with a fuselage of triangular section, both of the same height,  $h = 10$  cm. The lateral angles between wing and fuselage were given values of  $120^\circ$ ,  $90^\circ$ ,  $60^\circ$ , and  $45^\circ$  by changing the position of the fuselages which were sharp-edged and made a longitudinal angle of  $0^\circ$  with the wing (Figs. 9-12).

The result is shown by Fig. 13. Polar 3 for a fuselage with an angle of  $90^\circ$  shows only a small additional induced drag as compared with polar 1 (wing alone). The position of polar 2 for an angle of  $120^\circ$  is slightly worse, probably on account of the changed position of the center of pressure, which is shifted forward in this case.

Polar 4 of the model for an angle of  $60^\circ$  resembles the polar of a wing with a very poor aspect ratio. It approaches the maximum value of the wing alone. However, for the same angle of attack the lift coefficients steadily decrease. According to streamline investigations the flow begins to separate at the wing root at an angle of attack of approximately  $1.5^\circ$ . The flow actually separated along one-fifth of the span at an angle of attack of  $5.7^\circ$ .

This phenomenon is accounted for by the rapid expansion of the wedge-like spaces between the rear portion of the upper surface of the wing and the sloping sides of the fuselage. At these points the wing and the sides of the fuselage act like

diffusers. Figures 9-12 show how the lines of intersection of the upper surface of the wing and the sides of the fuselage recede from one another in the rear portion of the wing.

Hence the flow on the upper surface of the wing has to move against an extraordinarily high increase in pressure. The kinetic energy of the flow is not sufficient to overcome this increase in pressure, especially since, for small angles, the same frictional forces act on smaller volumes of air and the flow separates. As a result, the lift, otherwise uniformly distributed over the wing, is split up and causes an excessive increase of the induced drag.

Polar 5, angle of  $45^{\circ}$ , compares still more unfavorably with polar 4, angle of  $60^{\circ}$ . The expansion of the above-mentioned diffuser-like spaces is further augmented by the increasing reduction of the angle between the fuselage and the upper surface of the wing. Even at the angle of attack of vanishing lift, the flow separates at one-fifth of the span. At an angle of attack of  $2^{\circ}$  the vortex at the wing root is so strong that it extends over the lateral fuselage edges and likewise causes the flow to separate there. Even the flow less affected by the wing is broken at the largest angles of attack by the lateral edges of the rear portion of the fuselage. This finally leads to a flow about the fuselage, S-shaped as seen from the side, which accounts for the surprisingly great additional drag of polar 5.

## Series V.

## Fuselages Alone from Series IV

In confirmation of the fact that the high drag values of the polars for acute angles were not due to the fuselages alone, these were measured separately. The datum surfaces for the evaluation are the cross-sectional areas of the fuselage. The area of the square section of  $0.01 \text{ m}^2$  is the twentieth, and that of the triangular fuselage approximately the fortieth part of the datum surface of the "wing-and-fuselage" model. The moment axis passes through the nose of the fuselage. The datum depth is in each case the height of the fuselage  $h$ . In the case of the triangular fuselage, the angle of attack  $\alpha$  is negative when the sloping sides are first struck by the air flow.

The polars are shown in Figure 14. As was to be expected, the polars of the different fuselages differ only slightly, when the drag coefficients are converted to the datum area of the complete models. Up to an angle of attack of  $10^\circ$  the drag coefficients then agree fairly well with the additional drags which, in the preceding series of tests, constituted the difference between polar 2 (wing with square fuselage, vertical sides) and polar 4 (wing alone). Thus the fuselage alone does not account for the great drag of the "wing-and-fuselage" polar.

## Series VI.

## Models with Various Wing-Root Shapes

The next step, after determining the separation phenomena described in the fourth series of tests, was to work out a wing-root shape which, in spite of acute angles, would prevent the flow from separating. Two models of the fourth series of tests were used for the following tests. A new wing-root shape was obtained by filling out the diffuser above the rear portion of the wing root. This filling-out can be regarded as a rounding of the angle between the upper surface of the wing and the side of the fuselage, so that the radius of the rounded portion generally increases toward the rear.

In the case of the model with an angle of  $45^{\circ}$ , four polars with four different wing-root shapes were plotted. The shapes of the wing roots are shown in Figure 15.

The polars are plotted in Figure 16. The diagram also contains curves, derived from the fourth series of tests, for the "wing alone" (curve 1) and for the "wing and square fuselage" with vertical sides on the one hand and with vertical diagonals on the other hand (curves 2 and 3). Contrary to polar 3, polar 4 of the model with a "small rounding" (I in Fig. 15), characterized by a comparatively small radius of the rounded portion which increases toward the rear, very closely approached, up to approximately  $c_a = 0.85$ , the polar of the model with vertical sides. At  $c_a = 0.85$  the polar bends sharply to the right as

a result of the flow separating at the wing root. Polar 5 of the model with a "medium rounding" (II) is a further improvement over polar 4, inasmuch as the separation first occurs at  $c_a = 1.1$ . Lastly, on account of its small  $c_w$  values, polar 6 of the model with a "large rounding" (III) nearly touches polar 2 of the model without disturbance of the flow at a  $c_a$  of about 0.8. There are no sudden deflections, as in the case of the foregoing polars.

Polar 7 of the model with "wrong rounding" (IV), characterized by a comparatively large radius of the rounding, constant over the rear portion of the wing root, bends very strongly to the right at  $c_a = 0.75$  and soon exceeds the  $c_w$  values of polar 3 of a model without special root shaping. The "wrong rounding" is associated with a thickening of the wing-root sections and hence causes an expansion of the diffuser. This expansion accounts for the bending of the polar.

Two polars were plotted for the model with an angle of  $60^\circ$  and various wing-root shapes. The roundings are shown in Figure 17 and the polars in Figure 18. The diagram also contains polars of the "wing alone" (curve 1) and of the low-wing monoplane with triangular fuselage placed edge upward (curve 2) and edge downward (curve 3).

Again the polars obviously show the advantage gained by filling out the diffuser. In the upper portion of polar 5 the  $c_w$  values are even smaller than those of the polar with angles

of  $120^{\circ}$ , and the maximum lift is greater. Attention is again called to the absence of bends in the polars.

The above wing-root type can be used on full-sized airplanes to prevent separation of the air flow, as in the case of streamlined engine nacelles on the upper surface of the wing. In this connection, however, we wish to point out that a running propeller will probably lessen the separation of the air flow, especially when the propeller is located behind the diffuser.

#### Series VII.

##### Models with Trailing-Edge Cutaway

It might be thought that, in addition to filling in the diffuser at the wing root, a cutaway trailing edge of the wing would help to prevent the separation of the air flow, since the cutaway eliminates the diffuser.

In order to reach a good agreement with conditions in actual practice, a fuselage with a circular cross section and a wing with a No. 436 Göttingen section of medium thickness were selected for a corresponding series of tests. The aspect ratio of the wing was again 5, and the chord 16 cm. The fuselage was streamlined. The principal dimensions of the model are given in Figure 19. The cutaway portion of the wing was successively given three different shapes and its angles were semicircularly rounded off. The angle between wing and fuselage was  $3.2^{\circ}$ . The datum area for the evaluation is that of the wing alone without cutaway.

In Figure 20 the polar diagram for the "wing alone" shows the previously mentioned increase in profile drag with increasing size of the cutaway. The "large cutaway" is particularly detrimental. Although having a small span, it is very deep and reaches nearly to the leading edge of the section. The induced drag is greatly affected by this large cutaway.

There is a sudden, marked bend to the right, for a  $c_a$  of 0.55, in the curves for a fuselage and wing with cutaway (Fig. 21), which shows that the separation of the flow has not been prevented. The bend increases as the curves shift to the left, i.e., with diminishing cutaways. After the bend, the curves are remarkably straight. The same fact was observed for the curves of a wing with leading-edge cutaways, as shown on page 93 of Report II, of the Ergebnisse der Aerodynamischen Versuchsanstalt zu Göttingen. The lift distribution was again split up by action of the fuselage.

Figure 22 shows the pressure distribution over the wing section No. 389, which closely resembles section No. 436. A similar curve is obtained for the pressure distribution over a wing with cutaway trailing edge, except that the rear point of the pressure diagram is cut off. Consequently, there is a great increase of pressure above the narrow wing bridge and the turbulent zone behind the trailing edge of the cutaway section acts, in the case of a wing with fuselage, upon the whole wing bridge, where it causes the flow to separate.

In conclusion, it should be said that this article does not claim to exhaust the subject of mutual interference between wing and fuselage. It is thought, however, that the most important points of the problem, at least in so far as regards its experimental side, have been elucidated.

Translation by W. L. Koporinde,  
Paris Office,  
National Advisory Committee  
for Aeronautics.

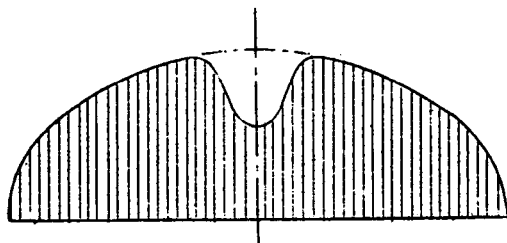


Fig.1 Disturbed lift distribution.

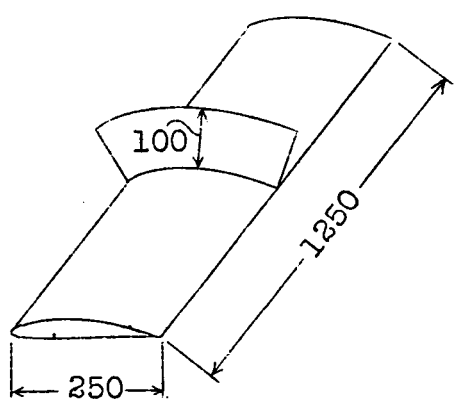


Fig.2 Wing with fuselage replaced by disk.

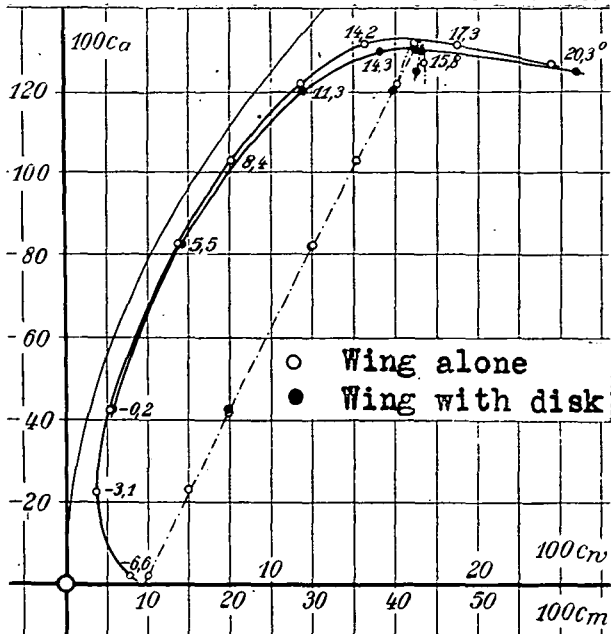


Fig.3 Wing with disk.

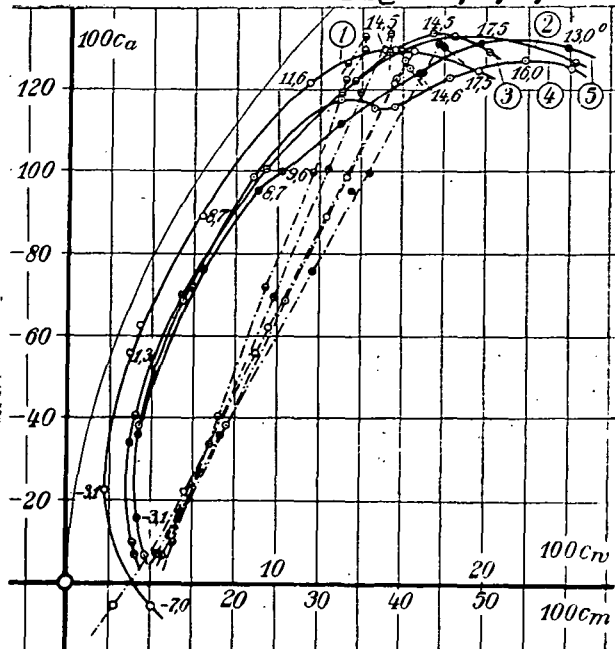
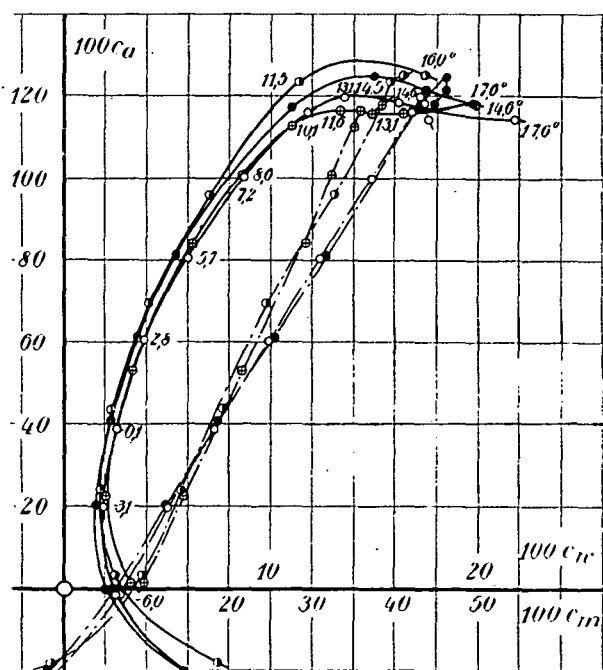


Fig.5 Wing at various distances from the nose of the fuselage.



- Tapered wing alone.
- " " with fuselage.
- Rectangular wing alone.
- " " with fuselage.

Fig.8 Fuselage with rectangular and tapered wings.

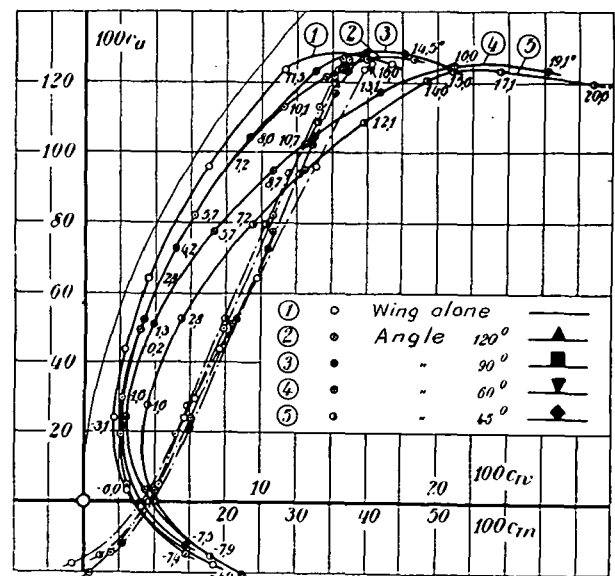


Fig.13 Wing with fuselage at various angles.

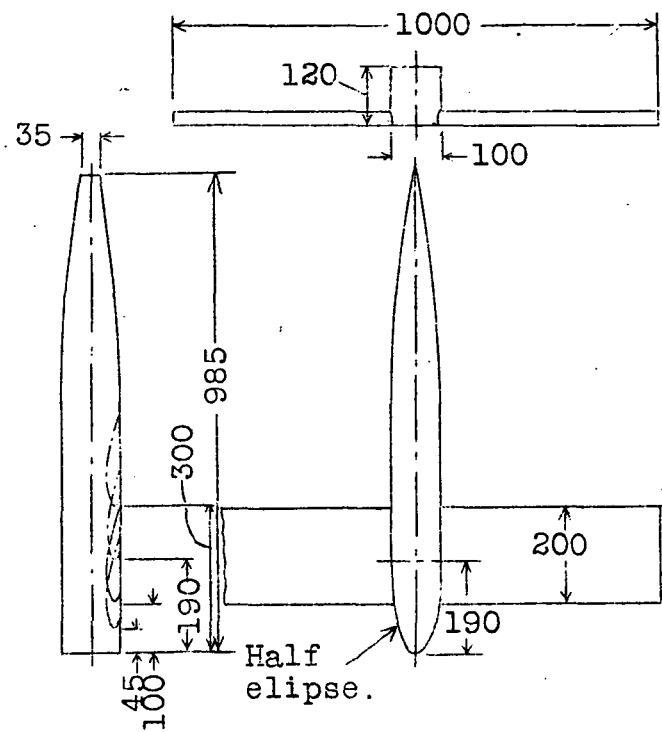


Fig.4 Wing at various distances from the nose of the fuselage.

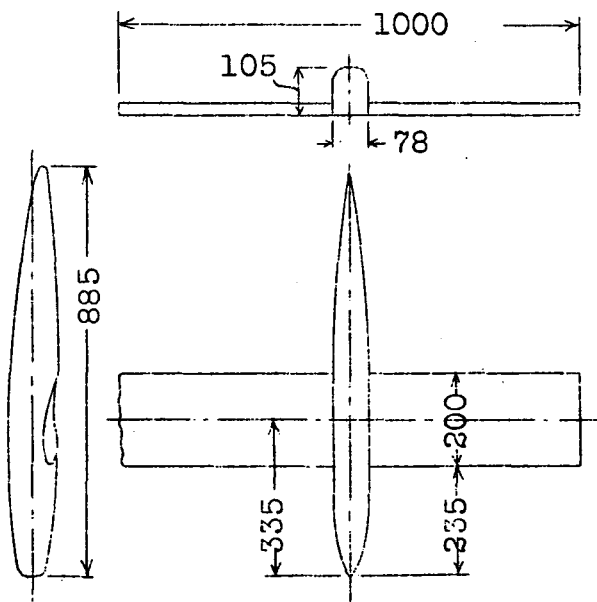


Fig.6 Fuselage with rectangular wings.

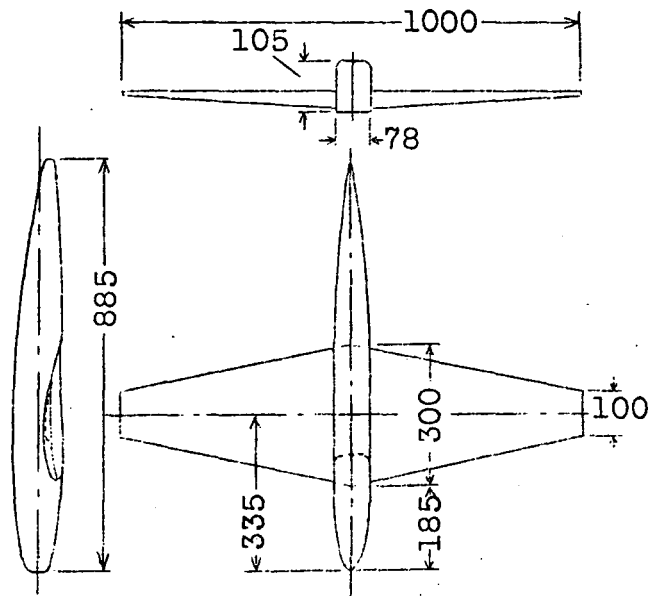


Fig. 7 Fuselage with tapered wings.

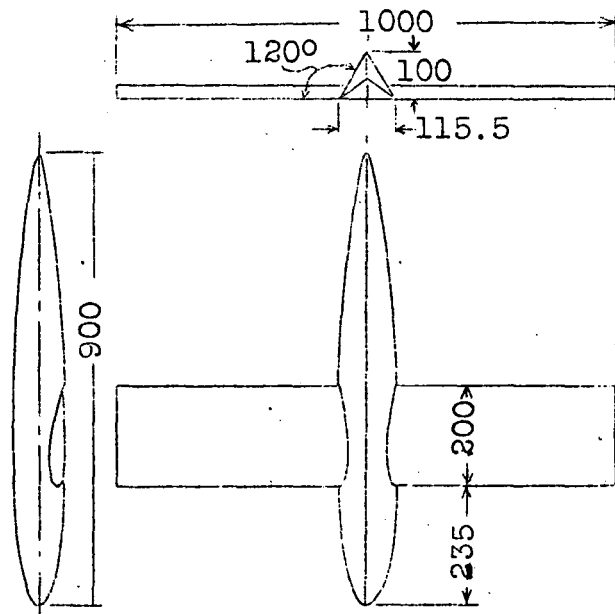


Fig. 9 Wing with triangular fuselage, angle 120°.

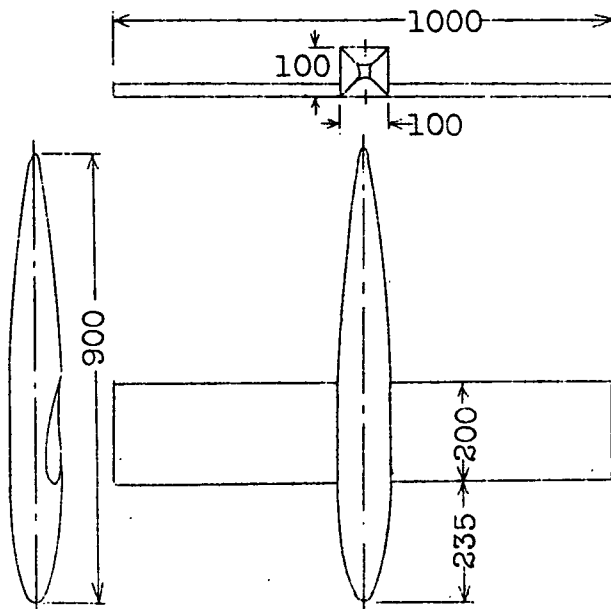


Fig.10 Wing with square fuselage, angle  $90^\circ$ .

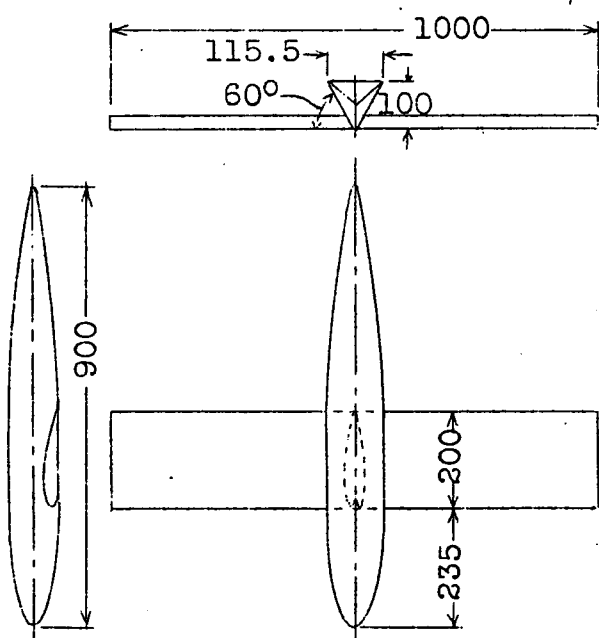
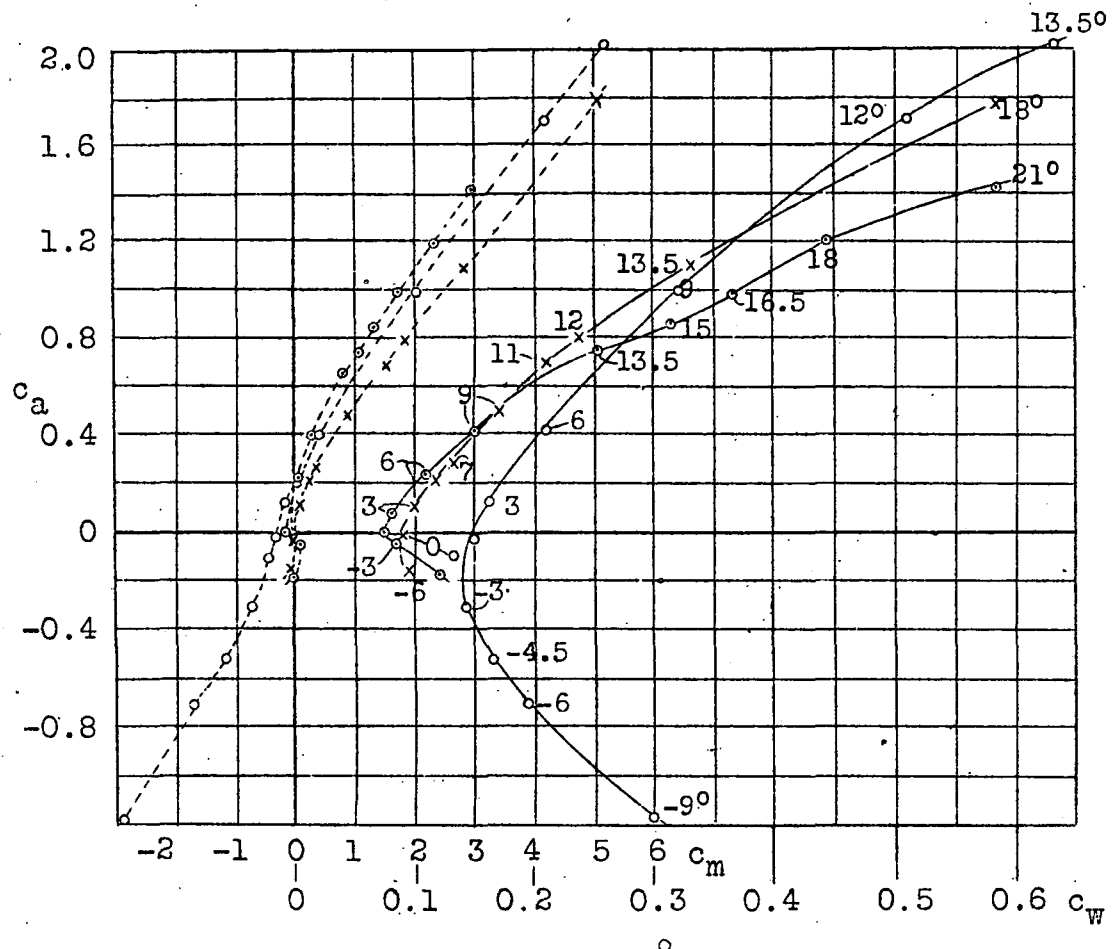


Fig.11 Wing with triangular fuselage, angle  $60^\circ$ .



○ Triangular fuselage  
 ○ Square fuselage, sides  $90^\circ$  position.  
 × " " " "  $45^\circ$  "

Fig.14 Fuselage alone.

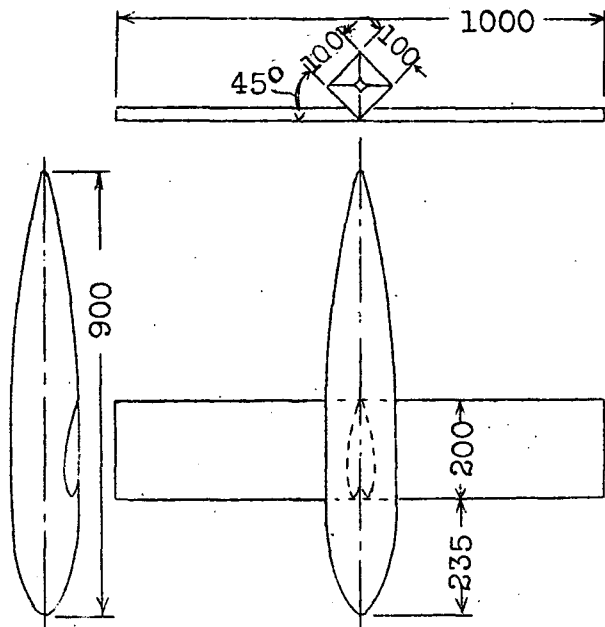


Fig.12 Wing with square fuselage, angle 45°.

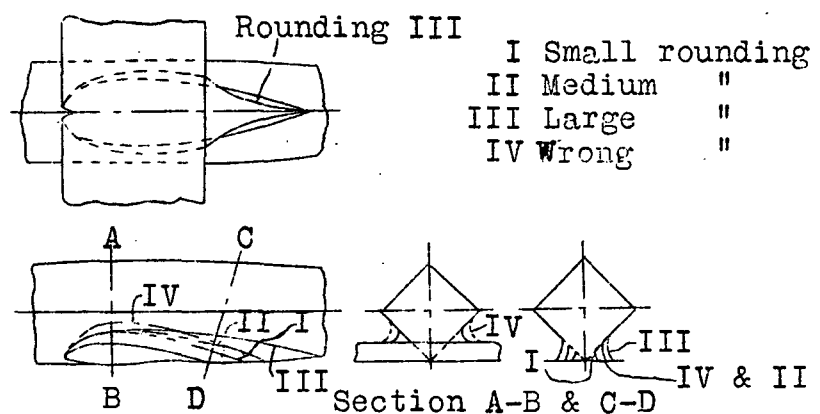
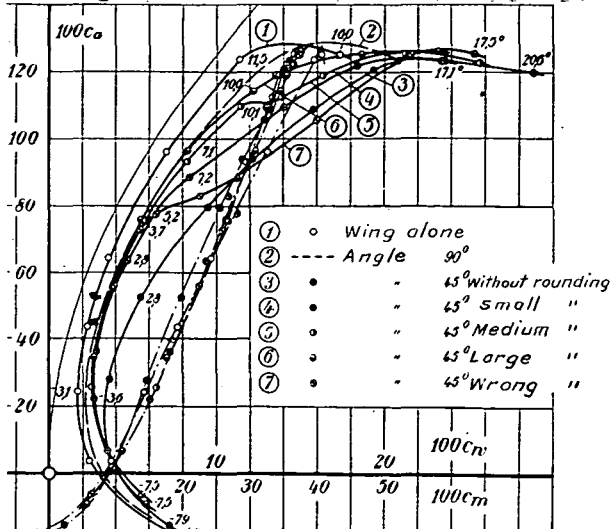
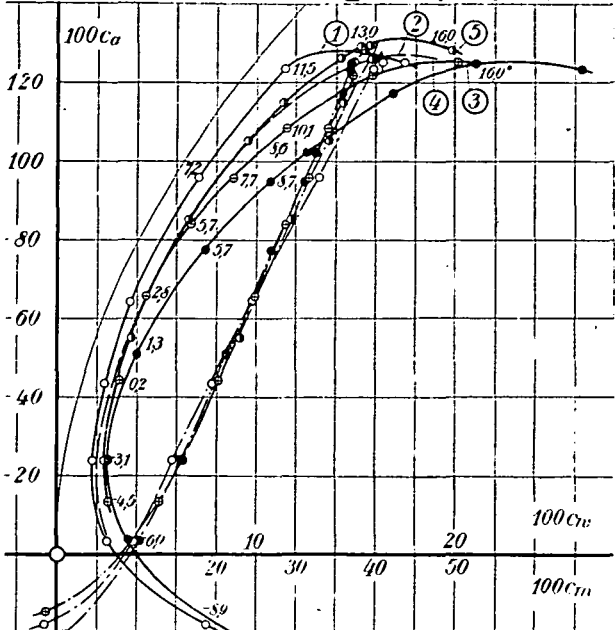
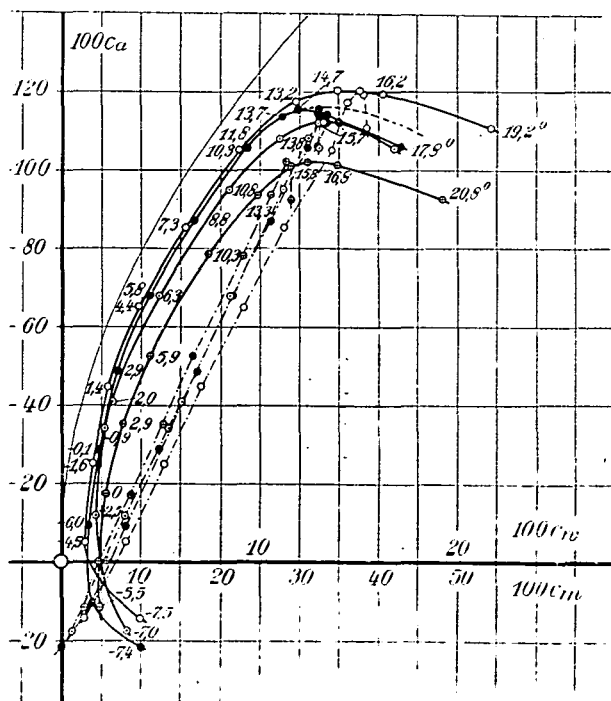


Fig.15 Angle of 45° with roundings.

Fig.16 Angle of  $45^{\circ}$  with roundings.

- (1) ○ Wing alone
- (2) --- Angle 1200
- (3) ● " 60° Without rounding
- (4) + " 60° Medium "
- (5) ● " 60° Large "

Fig.18 Angle of  $60^{\circ}$  with roundings.

- Wing without cutaway
- Wing with small "
- " medium "
- + " large "

Fig.20 Wing alone with cutaway.

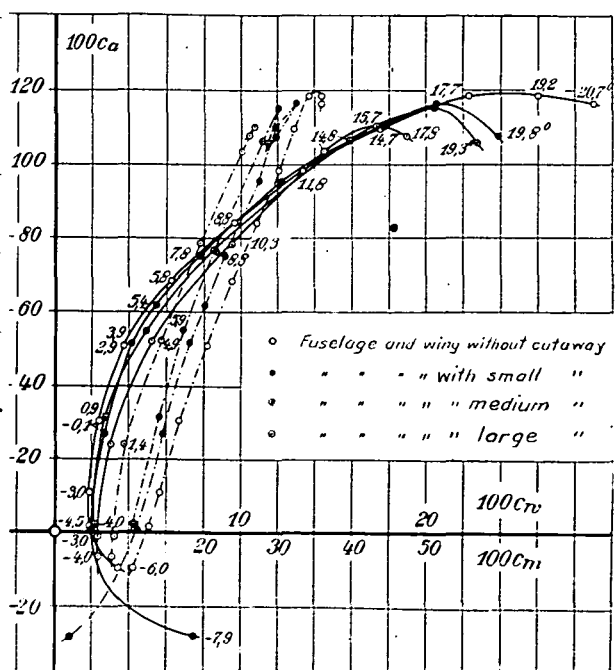


Fig.21 Fuselage and wing with cutaway.

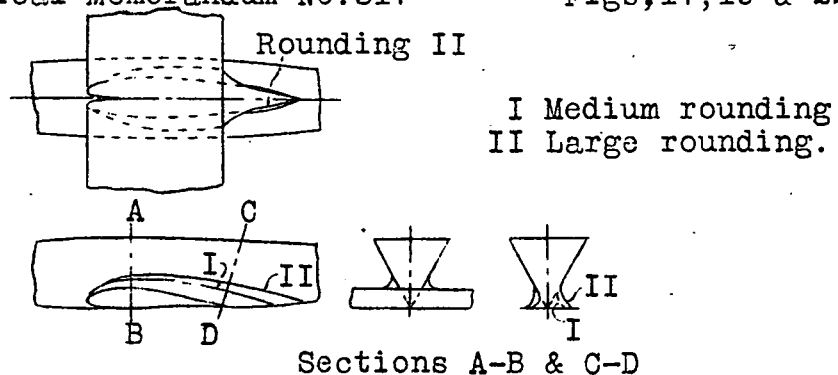
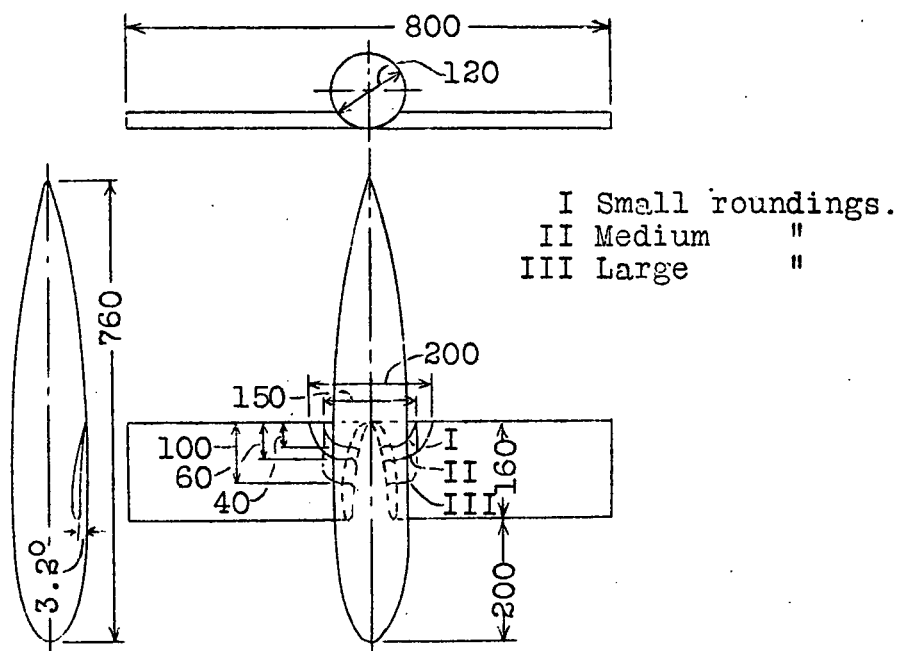
Fig.17 Angle of  $60^{\circ}$  with roundings.

Fig.19 Fuselage and wing with cutaway.

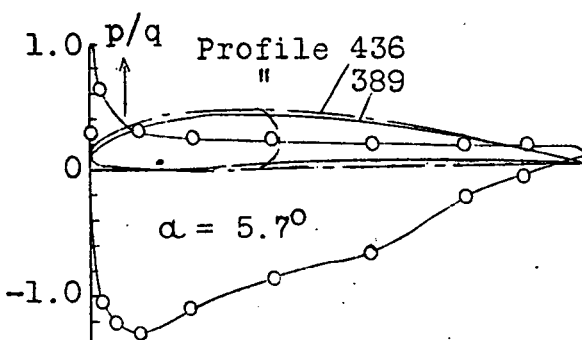


Fig.22 Pressure distribution on profile 389.